Journal of Cranio-Maxillo-Facial Surgery 43 (2015) 2129–2135

Contents lists available at ScienceDirect

Journal of Cranio-Maxillo-Facial Surgery

journal homepage: www.jcmfs.com

Positron emission tomography–computed tomography versus positron emission tomography–magnetic resonance imaging for diagnosis of oral squamous cell carcinoma: A pilot study

Tilo Schlittenbauer [a, *], Martin Zeilinger [b], Emeka Nkenke [c], Sebastian Kreißel [a], Matthias C. Wurm [a], Michael Lell [b], Torsten Kuwert [d], Michael Beck [d]

[a] Department of Oral and Maxillofacial Surgery (Head: Prof. Dr. F.W. Neukam), University of Erlangen-Nürnberg, Erlangen, Germany
[b] Department of Radiology, University of Erlangen-Nürnberg, Erlangen, Germany
[c] Department of Cranio-, Maxillofacial and Oral Surgery, University of Wien, Wien, Austria
[d] Clinic of Nuclear Medicine, Friedrich-Alexander-University Erlangen-Nürnberg, Erlangen, Germany

ARTICLE INFO

Article history:
Paper received 24 June 2015
Accepted 26 August 2015
Available online 11 September 2015

Keywords:
Positron emission tomography
Magnetic resonance imaging
Computed tomography
Head and neck neoplasms
Mouth neoplasms

ABSTRACT

Diagnostic imaging of head and neck cancer has made enormous progress during recent years. Next to morphological imaging modalities (computed tomography [CT] and magnetic resonance imaging [MRI]), there are also hybrid imaging systems that combine functional and morphological information (positron emission tomography [PET]/CT and PET/MRI). The aim of this study was to compare the diagnostic accuracy of PET/MRI in the diagnosis of head and neck cancer with other imaging modalities (MRI, CT, PET/CT). Ten patients (nine male and one female) with histologically proven oral squamous cell carcinoma participated in an 18 F-FDG-PET/CT scan and an additional 18 F-FDG PET/MRI scan prior to surgery. The morphological and functional results were compared with the histological results. Inclusion criteria were histologically proven oral squamous cell carcinoma and no prior surgical intervention, medical therapy, or local external radiation. There was no significant correlation between tumor differentiation and maximum standard uptake values. Functional imaging showed a slightly better correlation with the measurement of the maximal tumor diameter, whereas pure morphological imaging showed a better correlation with the measurement of infiltration depth. Only with PET/MRI could correct lymph node staging be reached; the other imaging tools showed false-negative or false-positive results. In conclusion, we showed in our limited patient cohort that PET/MRI is superior to the morphological imaging modalities, especially for lymph node staging.

1. Introduction

Malignant neoplasms of the head and neck region have occurred increasingly in the last few years. With an incidence of 650.000 and a mortality of 350.000 in Europe, they count for two to four percent of all known malignancies (Platz et al., 1983). The number of newly diagnosed disease varies throughout Europe, and numbers in southern Europe are higher than in the northern and central continent. According to statistics, each year 10–20 out of 100.000 people in Germany fall ill with head and neck neoplasms (Guntinas-Lichius et al., 2010). Disease usually occurs between the age of 50 and 60 years, and men are affected more frequently than women (Platz et al., 1983). One out of two patients dies within 5 years after the diagnosis of a carcinoma of the oral cavity. Most likely due to the late diagnosis, mortality has not changed significantly in recent years. Preventive measures and early diagnosis are the only proven determining factors that could lead to a higher 5-year-survival (Christoph, 2006). It has been reported that tumor size correlates with incidence of cervical metastases (Ermer et al., 2015).

Risk factors such as alcohol abuse and smoking cause up to 75% of oral squamous cell carcinoma. Betel nut chewing is another risk factor; it is not very common in Europe, but it is very popular in Asia and India (Zienolddiny et al., 2004).

Symptoms of head and neck neoplasms are various due to location and tumor stage. Early-stage cancer is usually quite asymptomatic.

* Corresponding author. Department of Oral and Maxillofacial Surgery, University of Erlangen-Nürnberg, Glückstrasse 11, 91054 Erlangen, Germany. Tel.: +49 9131 8534201; fax: +49 9131 8534219.
E-mail address: Tilo.schlittenbauer@uk-erlangen.de (T. Schlittenbauer).

http://dx.doi.org/10.1016/j.jcms.2015.08.030
1010-5182/

The fundamental diagnostic is a detailed anamnesis and thorough clinical examination. The clinician can gather information about tumor genesis and first indication for localization.

Endoscopic examinations combined with biopsy are also essential. Especially for the diagnosis of loco-regional lymph node metastasis, biopsy and pathological examination are seen as the gold standard (Quick et al., 2013; Rogers et al., 2004).

There are numerous imaging modalities. Sonography, angiography, scintigraphy, magnetic resonance imaging (MRI), computed tomography (CT), and positron emission tomography (PET) are often used in diagnostics.

Multidetector computed tomography is frequently used in preoperative staging and follow-up (Yamashina et al., 2008). Recent studies have evaluated its benefits in the control of resection margins (Feichtinger et al., 2010) or for image-guided endoscopic navigation (Feichtinger et al., 2007). It offers a short examination time and is therefore suitable for patients with late-stage neoplasms who may have dysphagia or compromised respiratory function (King, 2007). In the absence of metal artifacts, CT is able to illustrate the depth of infiltration, metastasis, and local bone infiltration, unlike PET (King, 2007; Sadick et al., 2012). Morphological changes after radiochemotherapy, flaps, or neck dissection can make image analysis quite difficult (Aschenbach and Esser, 2010; Sham and Nishat, 2012). Another domain is the diagnosis of neoplasms with infiltration of bone structures such as the orbit or base of the skull (Stuck et al., 2012; Zinreich et al., 1987).

Modern MRI offers high-resolution data within a reasonable time (Antoch et al., 2003). Furthermore it offers excellent soft tissue differentiation, which facilitates the assessment of local infiltration as well as perineural tumor spread. MRI is less susceptible to metal dental hardware and therefore is preferred in staging oral cavity or oropharyngeal cancer (Wolff et al., 2012).

PET scans produce images of metabolic processes in the body by detecting pairs of gamma-ray emitted by a tracer such as F-18-FDG. As it illustrates glucose utilization, even micro-metastases are detectable (Subramaniam et al., 2010).

The introduction of PET–CT as a hybrid imaging device in the middle of the last decade has allowed combining both functional and anatomical information, leading to better accuracy in oncological diagnoses than with stand-alone PET (Antoch et al., 2004). PET–CT has been recommended for staging, distant and micrometastasis detection, relapse, and cancer of unknown primary detection as well as IMRT planning (Reske and Kotzerke, 2001).

Relapse is usually found within the first 2 years after diagnosis, and morphological information from MRI or CT scans might be difficult to interpret in many cases (Herrmann et al., 2009; Hustinx and Lucignani, 2010; Levine et al., 2011; Yaghmai et al., 2011).

The latest development in the field of PET was the establishment of PET–MRI, providing metabolic information together with superior soft tissue contrast of MRI (Antoch and Bockisch, 2009). Another study presented the successful use of PET/CT/MRI in minimally invasive biopsies (Reinbacher et al., 2014).

The aim of the current study was to compare the diagnostic accuracy of PET/MRI with other imaging modalities (MRI, CT, PET/CT) in the diagnosis of head and neck cancer, with the eventual aim of reaching a diagnostic standard.

2. Material and methods

2.1. Patients

This prospective study was performed with ethics committee approval between June and September 2013. Ten patients (nine male and one female, median age 61.3 years, range 45–79 years) with oral squamous cell carcinoma prior to surgery were included after consenting to study participation. Inclusion criteria were as follows: histologically proven oral squamous cell carcinoma; no prior surgical intervention, medical therapy, or local external radiation; no contraindications to one of the imaging modalities (Contrast medium (CM) allergy, implanted electrical devices, claustrophobia); and no uncontrolled serum glucose levels.

2.2. Data acquisition

All patients fasted for at least 4 h prior to the investigation. A mean dose of 222.5 ± 46.6 MBq (6.01 ± 1.25 mCi) fluor-18-deoxyglucose was injected prior to PET/CT scan. All patients underwent a standard protocol PET/CT scan on a Siemens Biograph mCT hybrid scanner (Siemens Healthcare Sector, Erlangen, Germany) with an axial field of view (FOV) of 21.6 cm a mean of 66 ± 6.7 min after injection. All patients were scanned for 3 min per bed position in seven to eight bed positions from head to mid femur. Subsequently patients were scanned on a Biograph mMR hybrid PET/MRI scanner (Siemens Healthcare Sector, Erlangen, Germany). The Biograph mMR combines 3.0-T a whole-body MR device with a fully integrated PET detector ring and an axial FOV of 25.8 cm. MR and PET data are acquired simultaneously. The system is equipped with phased-array radiofrequency (RF) receiver coils (TIM, Total Imaging Matrix, Siemens Healthcare Sector, Erlangen, Germany), which cover the whole patient, featuring a rigid 16-channel head/neck coil. PET/MRI acquisition started 145.9 ± 20.6 min after FGD injection. A time delay of 79.9 ± 19.8 min resulted because of the necessary transportation of the patient from the PET/CT site to the PET/MRI site, which is not located in the same building. To account for the radioactive decay of the tracer, an acquisition time of 20 min in one bed position over the head/neck area was chosen, as previously published (Abouzied et al., 2005).

2.3. MRI

A T2-weighted Turbo-Inversion Recovery-Magnitude (TIRM) sequence both in axial (FOV 240 × 240 mm, matrix 224 × 320, ST 3 mm, 1 average, TR 5311 ms, TE 40 ms) and coronal orientation (FOV 260 × 260 mm, matrix 320 × 224, ST 4 mm, 1 average, TR 4400 ms, TE 40 ms), a T1 weighted turbo-spin-echo (TSE) sequence in axial orientation covered the head and neck area (FOV 220 × 220 mm, matrix 320 × 256, ST 2 mm, 1 average, TR 5.77 ms, TE 2.46 ms). After CM injection, a series of T1 Dixon Volume Interpolated Breathhold Examination (VIBE) in axial (FOV 220 × 220 mm, matrix 320 × 272, ST 2 mm, 1 average, TR 8.16 ms, TE 4.92 ms) and coronal orientation (FOV 260 × 260 mm, matrix 320 × 192, ST 4 mm, 2 averages, TR 637 ms, TE 14 ms) were acquired, followed by axial fat saturated T1 weighted TSE (FOV 177 × 320 mm, matrix 320 × 272, ST 3 mm, 2 averages, TR 8.16 ms, TE 4.92 ms). Furthermore diffusion-weighted sequences in axial orientation of the head and neck region as well as the whole body were performed (FOV 374 × 380 mm, matrix 138 × 136, ST 6 mm, 4 averages, TR 1,23,000 ms, TE 78 ms).

2.4. Data processing

Reconstruction of the PET data used ordered-subsets expectations maximization (OSEM 3D) with three iterations and 21 subsets, no Gaussian filter was applied. Attenuation correction (AC) was made in PET/CT based on CT-derived data and Hounsfield units (HU) using standard software (Siemens Healthcare Sector, Erlangen, Germany) (Anneroth et al., 1986; Cancer, 1988). For PET/MRI, attenuation correction was based on Dixon VIBE sequences to

create an individual μ-map with tissue subclassification in three groups (fat, soft tissue, and lung tissue).

2.5. Image analysis

PET/CT and PET/MRI images were analyzed separately for tracer positive lesions by two nuclear physicians with 3 and 16 years of experience in PET image reading. Consensus was reached in all patients. Two experienced radiologist readers interpreted MRI and CT images. Image analysis was performed using dedicated workstations (Syngo Via, Siemens Healthcare, Erlangen, Germany). Standard uptake values (SUVs) were measured using isometric volumes of interest (VOIs) generated by the VOI function of the software. Regional tracer uptake was expressed as SUV max and SUV mean. Tumor extent in hybrid imaging was measured, due to a missing standard, on the common clinical window setting with an upper margin of SUV 5.0, with no background correction. Tumor boundaries were manually segmented to visually fit PET, CT, and MRI images, respectively. On CT and MRI, tumor dimensions were also drawn manually as seen by the physicians.

2.6. Statistical analysis

The nonparametric Wilcoxon signed-rank test was used to evaluate for significant median differences. Significance was accepted for $p < 0.05$. Nonparametric correlation was analyzed via the Spearman rho test. Overall agreement was rated using Cohen's kappa. Significance was accepted for $p < 0.05$. Statistical analyses were carried out using IBM SPSS Statistics version 19 (IBM, Armonk, NY).

3. Results

3.1. Primary lesion

All patients had squamous cell carcinoma, which, in one case was well, in four cases moderately, and in five cases poorly differentiated. We did not find any significant correlation between differentiation and maximum standard uptake value (SUV max). The SUV max was 14.1 ± 3.2 for PET/CT and 14.2 ± 4.6 in PET/MRI, respectively. There was no significant difference between the measured SUV in PET/CT and PET/MRI ($p = 0.79$). On the other hand, a high correlation using the two-sided Spearman rho test ($r = 0.68$, $p = 0.03$) was observed. The small observed differences in tumor FDG uptake are most commonly a result of the sequential acquisition mode and therefore a metabolic disparity in PET/MRI compared to PET/CT (Abouzied et al., 2005). Mean standard uptake values (SUV mean) showed comparable results, with a SUV mean of 8.1 ± 2.1 in PET/CT and 8.6 ± 3.1 in PET/MRI. The results of SUV max and SUV mean, depending on tumor differentiation, are shown in Table 1.

The maximal tumor diameter and infiltration depth were measured in PET/CT and PET/MRI as well as in CT and MRI alone. Compared to the histological results, hybrid imaging did not significantly differ from histological measurement in relation to diameters ($p = 0.34$), but there was a considerable disagreement between pathological finding and the results of CT and MRI ($p = 0.018$ and $p = 0.018$, respectively). The results are also shown in Table 2 and Graph 1.

As shown in Table 2 and Graph 2, infiltration depth on the other side could not be predicted by functional imaging. Compared to the later retrieved histological results, a significant difference was observed for both PET/CT and PET/MRI, respectively ($p = 0.017$ and $p = 0.018$). Morphological imaging showed a better correlation with pathological findings ($p = 0.12$). A general overestimation of tumor infiltration in functional imaging of the mouth base was observed.

3.2. Lymph node staging

Histology proved lymph node metastasis in five of nine patients. One patient underwent combined radio- and chemotherapy instead of surgery, with no histological proof of lymph node metastasis available. This patient was excluded from statistical analysis. In FDG PET/CT, lymph nodes in four patients were evaluated as suspected metastases, five in PET/MRI, four in CT, and seven in MRI stand-alone. The SUV max of suspected lymph node metastasis measured 4.4 ± 0.7 with a range of 2.5–11.2 in PET/CT, and 5.7 ± 0.8 with a range of 2.8–11.2 in PET/MRI, respectively. A significant difference between the SUV max of both methods could be found ($p = 0.015$). The SUV mean was 2.6 ± 0.4 and 3.2 ± 0.5 in PET/CT and PET/MRI. There was no significant difference between methods ($p = 0.24$). Compared to the histology, PET/CT showed two false-negative results, CT one false-negative result, and MRI three false-positive results. Only in PET/MRI was lymph node staging completely accurate. False-negative lymph nodes in PET/CT did not exceed 8 mm in short diameter and showed only a slight FDG uptake up to a SUV max of 2.0; they were rated as inflammatory lymph nodes. Overall agreement κ rated 0.83 ($p < 0.05$) in PET/CT, 1.0 ($p < 0.05$) in PET/MRI, 0.91 ($p < 0.05$) in CT and 0.65 ($p < 0.05$) in MRI, respectively. Due to the small number of patients, the sensitivity and specificity of the methods can be estimated only imprecisely, as shown in Table 3.

For lymph node localization, we used the classification published by Robbins. Suspected lymph node metastases were classified as follows 1) Level I; 2) Level II; 3) Level III; 4) Levels I and II; 5)

Table 1
Results of PET SUV measurements in depending on tumor rating.

Differentiation	No of patients	PET/CT SUV max	PET/MRI SUV max	PET/CT SUV mean	PET/CT SUV mean
Well (G1)	1	9.6	10.0	5.6	5.9
Moderately (G2)	4	14.4 ± 2.8	15.7 ± 4.2	8.2 ± 1.7	9.1 ± 2.7
Poorly (G3)	5	14.7 ± 4.0	13.8 ± 5.2	8.5 ± 2.5	8.8 ± 3.8

Table 2
Results of distance measurements.

Diameter PET/CT	Diameter PET/MRI	Diameter CT	Diameter MRI	Diameter histological finding
4.2 ± 1.0 cm	4.1 ± 0.8 cm	3.5 ± 0.8 cm	3.4 ± 0.8 cm	4.4 ± 0.8 cm
Infiltration PET/CT	Infiltration PET/MRI	Infiltration CT	Infiltration MRI	Infiltration histological finding
3.3 ± 1.0 cm	3.3 ± 0.8 cm	2.3 ± 1.1 cm	2.6 ± 1.0 cm	1.9 ± 0.9 cm

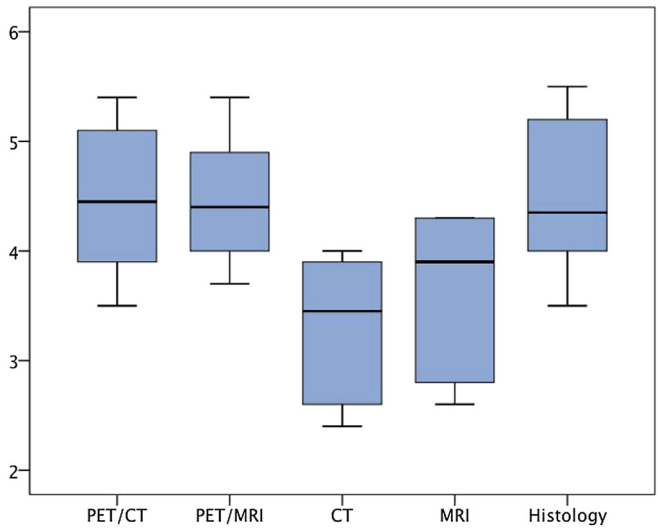

Graph 1. Boxplot of tumor diameter in centimeter measured on different modalities.

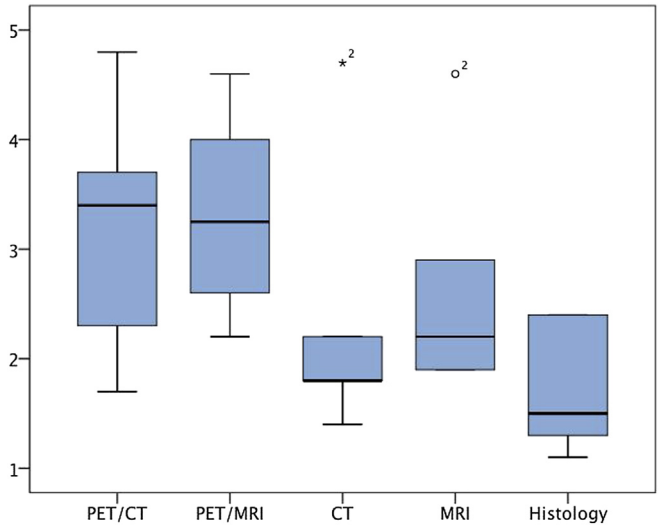

Graph 2. Boxplot of infiltration depth in centimeter measured on different modalities.

Table 3
Sensitivity, specificity and overall agreement κ for lymph node staging.

	PET/CT	CT	PET/MRI	MRI
Sensitivity	60%	80%	100%	100%
Specificity	100%	100%	100%	25%
Kappa	0.83	0.91	1.0	0.65

Levels II and III; 6) Levels I and III; and 7) Level I, II and III. They were then compared with the results of lymph node dissection. PET/CT showed correct results in six of eight cases, CT in seven of eight, MRI in five of eight, and PET/MRI in eight of eight cases, respectively. Overall agreement κ rated 0.74 ($p < 0.05$) for PET/CT, 0.87 ($p < 0.05$) for CT, 0.65 ($p < 0.05$) for MRI, and 1.0 ($p < 0.05$) for PET/MRI (Table 4).

4. Discussion

Individual personalized therapy concepts play a crucial role in the treatment of malignant head and neck tumors. Despite constant improvements in operational and diagnostic facilities, the survival rates have not improved significantly in recent years (Carvalho et al., 2005; Jemal et al., 2007). In addition to clinical and histopathological examination, various imaging technologies such as MRI and CT, which allow verification of the tumor by morphological and anatomical features, are necessary to determine the optimal therapeutic approach with the least therapy-induced comorbidity for the individual patient. Unfortunately, the clarification of tumor dignity with purely morphological methods is often difficult. Therefore, due to the additional metabolic information provided, such as increased glucose metabolism, such hybrid imaging methods as PET–CT and PET–MRI can improve our understanding of the disease (Subramaniam et al., 2010).

Table 4
Suspected location of lymph node metastases compared to post-surgical pathological results for each patient.

Patient-ID	Pathology	CT	MRI	PET/CT	PET/MRI
P001	None	None	None	None	None
P002	Level 2 + 3	None	None	None	Level 2 + 3
P003	None	None	None	None	None
P004	Level 2	Level 2	Level 2	None	Level 2
P005	None	None	Level 3	None	None
P006	Level 1 + 2	Level 1 + 2	Level 1 + 2	Level 1 + 2	Level 1 + 2
P007	None	None	Level 1	None	None
P008	Level 2	Level 2	Level 2	Level 2	Level 2

The aim of this study was to compare the diagnostic accuracy of PET/MRI with the other imaging modalities (MRI, CT, PET/CT) in the diagnosis of head and neck cancer, with the eventual aim of reaching a diagnostic standard. With regard to the assessment of the primary tumor, no diagnostic advantage of PET–MRI compared to PET–CT could be found (Fig. 1), which is in line with a previous report, with a matching rate of 97.4% between the two imaging methods (Quick et al., 2013). In another study, no significant difference in the diagnostic potential of the two methods was found (Kubiessa et al., 2014). Nakamoto et al. were able to show that the sensitivity could be increased by image fusion of MR images with the PET data sets. The sensitivity for the sole MRI scan was 98%, and after the image fusion rate reached 100% (Nakamoto et al., 2009). Furthermore, we demonstrated that morphological and functional imaging (PET–CT, PET–MRI) provide better correlation with respect to the assessment of tumor diameter, in comparison to the purely morphological methods. PET–CT showed the best correlation, closely followed by PET–MRI. A similar result was observed in another study (Huang et al., 2011).

In addition, the infiltration depth was determined with the imaging techniques and compared with the histopathological findings in this study. The purely morphological methods (CT, MRI) were superior to the morphological and functional methods (PET–CT, PET–MRI). The analysis of the PET–CT and PET–MRI images revealed that tumor infiltration was overstaged. One possible reason for the inadequate assessment by the morphological and functional methods (PET–CT, PET–MRI) is the physiological FDG uptake in the mouth and throat.

High physiological FDG uptake can be observed in Waldeyer's ring, active muscles (vocal cord movement, swallowing) salivary glands, and brown fat (Sadick et al., 2012, Abouzied et al., 2005; Cook et al., 2004; Nakamoto et al., 2005). Furthermore, there is increased FDG due to inflammatory reactions, for example in the area of tumorous tissue, which distorts the assessment of tumor infiltration.

Since tumor extent was measured manually, it was user dependent and influenced by the windowing used to visualize the images. A work by Hong et al. published in 2014 tried to estimate the influence of dental artifacts on tumor staging. To evaluate

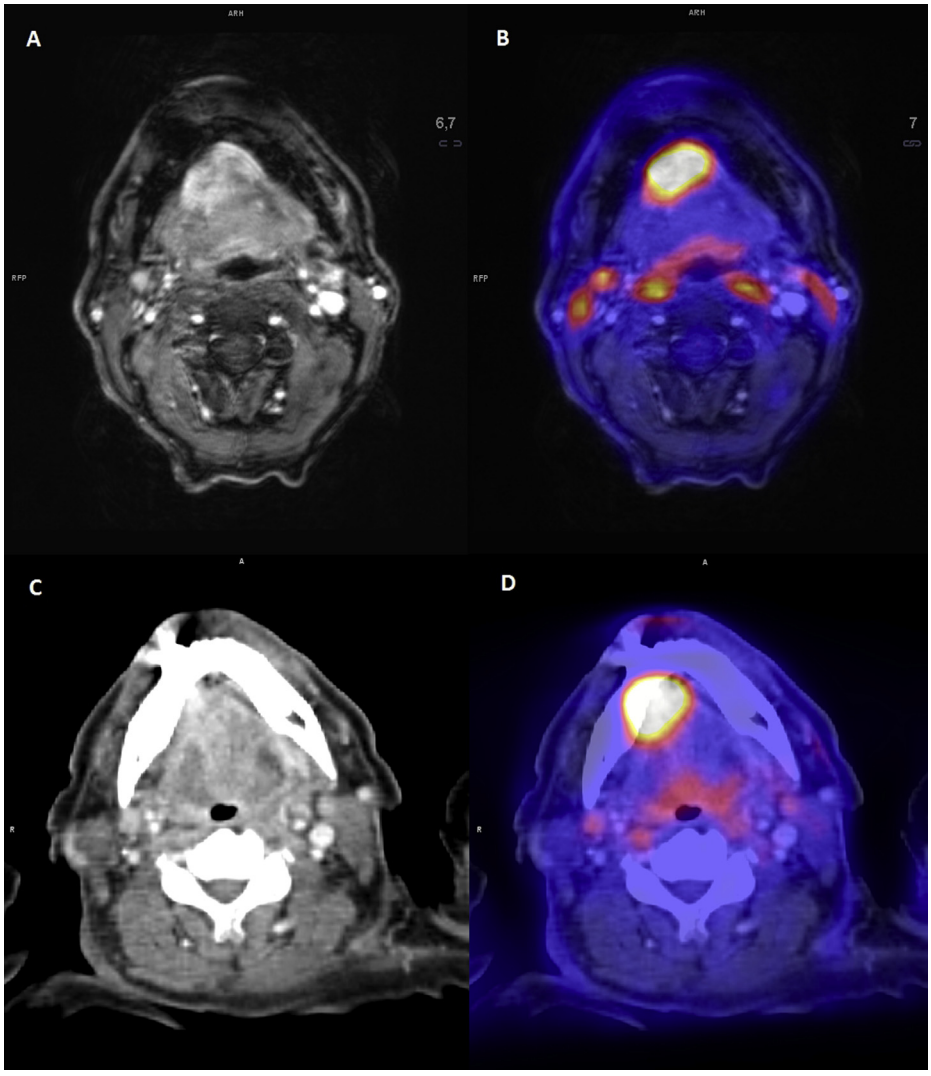

Fig. 1. Local oral squamous cancer of the tongue in PET/CT 64 min post injection and PET/MRI 121 min post injection A) T1w TSE DIXON contrast enhanced transversal B) Fused PET and T2w TSE native transversal C) CT B41s transversal contrast enhanced D) Fused PET AC and CT. Tumor extent cannot be distinguished in stand-alone CT due to metal artefacts and a more diffuse contrast enhancement. The neoplasm shows a good contrast enhancement in MRI, however image quality is reduced by motion artefacts. A high FDG uptake both in PET/CT and PET/MRI can be observed.

tumor extent in PET, these investigators used isometric VOIs and different cut-off values, yielding user-independent results (Hong et al., 2014).

Lymph node staging was most accurate in PET–MRI. For a long time, PET–CT has been used in the nodal staging of head and neck cancer. The importance of this modality was confirmed by numerous studies (Fletcher et al., 2008; Haerle et al., 2011; Higgins et al., 2012; Hustinx and Lucignani, 2010; Rodel et al., 2004; Subramaniam et al., 2010).

With a sensitivity of 87%–90%, a specificity of 80%–93%, and a negative predictive value (NPV) of 89%–95%, PET–CT can be successfully used for the initial nodal staging and relapse diagnosis of cervical lymph node metastases. In a study of 73 patients with different tumor entities, the diagnostic accuracies of PET–CT and PET–MRI were examined for TNM staging. There was no significant difference in the regional lymph node staging between the two forms (Fig. 2). Lymph node staging was performed correctly in 55 of 64 patients in the PET–CT group (82%) and in 56 of 64 patients in the PET–MRI group (84%). PET–CT had a sensitivity of 65%, a specificity of 94%, a positive predictive value (PPV) of 79%, a negative predictive value (NPV) of 89%, and a diagnostic accuracy of 87%. The corresponding values for the PET–MRI were 63%, 94%, 80%, 87%, and 85% (Heusch et al., 2015).

In this study, PET–MRI showed the best results regarding the staging of cervical lymph nodes. There are various explanations for this. One reason is that a better tumor-to-background-ratio results because of the longer acquisiton time of PET data in PET/MRI. Further studies should be conducted on this topic. The development of standardized examination protocols is of enormous importance for clinical use. Another possible reason for the superiority of PET–MRI in cervical lymph node staging is the fact that there is a time-dependent FDG uptake increase in tumor cells. Tumor cells show increased proliferation rates in addition to enzymatic changes. There is an increased expression of glucose transporters, for example GLUT1 and GLUT3 (Kurokawa et al., 2004). Furthermore vascular endothelial growth factor (VEGF)-activated endothelial cells have been found in tumors, which can lead to increased FDG uptake over time (Kostakoglu et al., 1996).

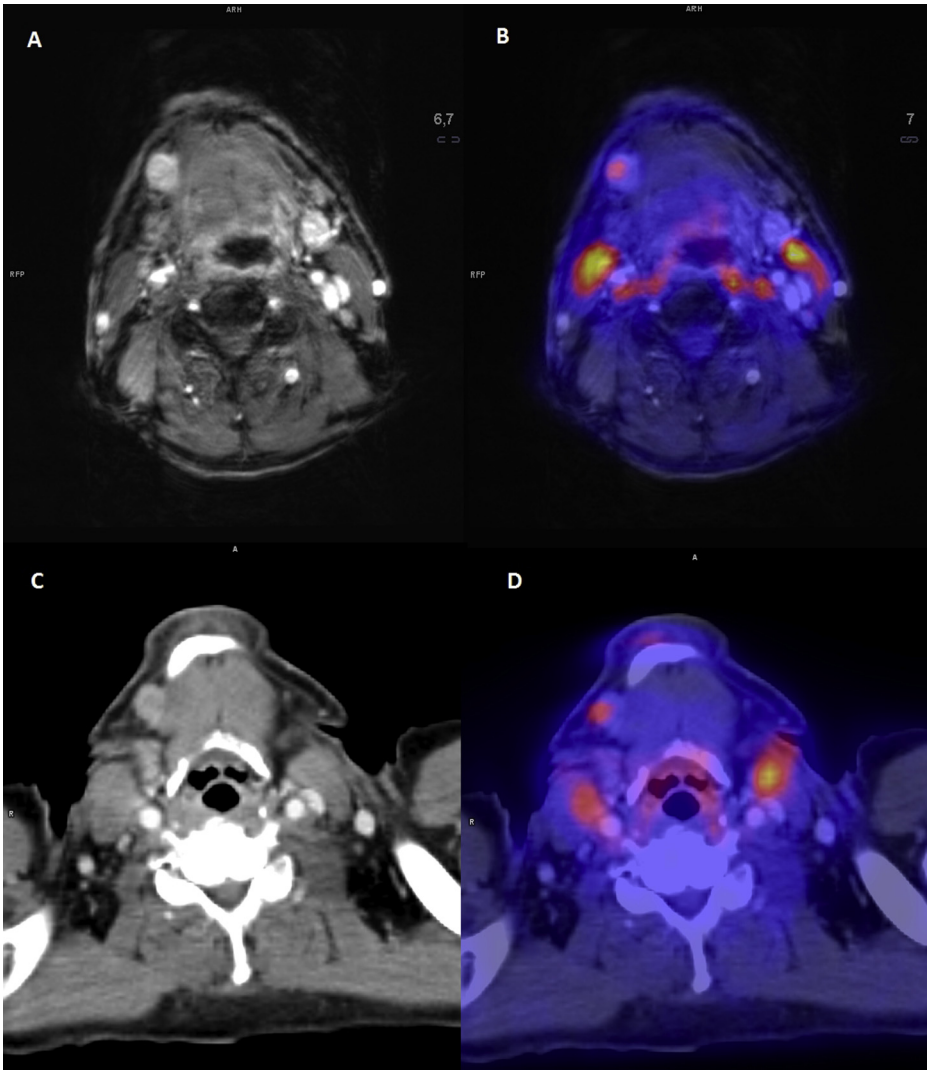

Fig. 2. Lymph node metastases in Level 2b right in PET/CT 64 min post injection and PET/MRI 121 min post injection A) T1w TSE DIXON contrast enhanced transversal B) Fused PET and T2w TSE native transversal C) CT B41s transversal contrast enhanced D) Fused PET AC and CT. A high contrast enhancement both in CT and MRI can be observed. MRI image quality is reduced by motion artefacts. Though FDG uptake is only slightly increased, the lesion was correctly classified as malign in both hybrid imaging modalities.

Another advantage of MRI compared to CT is the higher local resolution of lymph nodes and soft tissue as well as fewer artifacts caused by dental restorations. Tumors and metastases present better if located close to the mucosa, submucosa, salivary glands, and the base of the tongue (Sadick et al., 2012). This can be considered as another possible cause of the superiority of PET–MRI in cervical lymph node staging. The improved local tissue contrast of MRI shows its superiority in the complex anatomy of the head and neck region. Therefore MRI seems to be a candidate for the diagnosis of relapses. In this study, no patients with relapses were included. Therefore, future studies should investigate the potential of PET/MRI in terms of diagnosis of recurrent head and neck neoplasms.

A major limitation of the present study was the small number of patients. Subsequent studies need to include a larger number of patients to confirm the results obtained here. In addition, the variation in time between PET/CT and PET/MRI scans, with no possible time–activity curve extrapolation and thus an uncorrectable influence on tracer distribution, is a major drawback.

This study showed that the implementation of simultaneous PET–MRI imaging is possible and has yielded promising results. Especially in the staging of cervical lymph nodes, PET–MRI proved to be advantageous. The relatively young technology is still in its infancy and has great development potential. Further studies are needed to confirm the results, to achieve the eventual implementation of a clinical standard in the diagnosis of malignant neoplasms of the head and neck region. The clinical application of more tumor-specific tracers such as18-F-fluoro-α-methyltyrosine (18-F-FAMT) is in progress, which might overcome the main drawback of FDG, the nonspecific uptake in inflammation and organs of the oral cavity (Kim et al., 2015). In line with a recent study of Xiao et al., MRI seems to be an accurate tool in head and neck tumor diagnosis (Xiao et al., 2015).

5. Conclusion

These preliminary data suggest that PET/MRI might be advantageous in cervical lymph node staging of head and neck cancer. Further studies with more patients are needed to make reliable statements about the benefits of PET–MRI. In addition, various sequences should be checked for their usefulness in this specific question.

Conflict of interest

The authors declared that they have no competing interests with regard to this work. No grants were used.

References

Abouzied MM, Crawford ES, Nabi HA: 18F-FDG imaging: pitfalls and artifacts. J Nucl Med Technol 33: 145–155, 2005 quiz 162-143

Anneroth G, Hansen LS, Silverman Jr S: Malignancy grading in oral squamous cell carcinoma. I. Squamous cell carcinoma of the tongue and floor of mouth: histologic grading in the clinical evaluation. J Oral Pathol 15: 162–168, 1986

Antoch G, Bockisch A: Combined PET/MRI: a new dimension in whole-body oncology imaging? Eur J Nucl Med Mol Imaging 36(Suppl. 1): S113–S120, 2009

Antoch G, Saoudi N, Kuehl H, Dahmen G, Mueller SP, Beyer T, et al: Accuracy of whole-body dual-modality fluorine-18-2-fluoro-2-deoxy-D-glucose positron emission tomography and computed tomography (FDG-PET/CT) for tumor staging in solid tumors: comparison with CT and PET. J Clin Oncol: Official Journal of the American Society of Clinical Oncology 22: 4357–4368, 2004

Antoch G, Vogt FM, Freudenberg LS, Nazaradeh F, Goehde SC, Barkhausen J, et al: Whole-body dual-modality PET/CT and whole-body MRI for tumor staging in oncology. JAMA 290: 3199–3206, 2003

Aschenbach R, Esser D: Post-therapeutic imaging strategies and follow-up in head and neck malignant tumours. HNO 58: 749–755, 2010

Cancer: Manual for staging of cancer, 3rd ed. JB Lippincot, 1988 AJCO

Carvalho AL, Nishimoto IN, Califano JA, Kowalski LP: Trends in incidence and prognosis for head and neck cancer in the United States: a site-specific analysis of the SEER database. Int J Cancer Journal International du Cancer 114: 806–816, 2005

Christoph M: Risikoermittlung, Prävention und Früherkennung von Kopf- Hals-Karzinomen. Jahresversammlung der deutschen Gesellschaft für HNO Heilkunde, Kopf-und Hals-Chirurgen eV 77, 2006

Cook GJ, Wegner EA, Fogelman I: Pitfalls and artifacts in 18FDG PET and PET/CT oncologic imaging. Semin Nucl Med 34: 122–133, 2004

Ermer MA, Kirsch K, Bittermann G, Fretwurst T, Vach K, Metzger MC: Recurrence rate and shift in histopathological differentiation of oral squamous cell carcinoma – a long-term retrospective study over a period of 13.5 years. J Craniomaxillofac Surg 43(7): 1309–1313. http://dx.doi.org/10.1016/j.jcms.2015.05.011, 2015 Sep [Epub 2015 May 30]

Feichtinger M, Aigner RM, Santler G, Karcher H: Case report: fusion of positron emission tomography (PET) and computed tomography (CT) images for image-guided endoscopic navigation in maxillofacial surgery: clinical application of a new technique. J Craniomaxillofac Surg: Official Publication of the European Association for Cranio-Maxillo-Facial Surgery 35: 322–328, 2007

Feichtinger M, Pau M, Zemann W, Aigner RM, Karcher H: Intraoperative control of resection margins in advanced head and neck cancer using a 3D-navigation system based on PET/CT image fusion. J Craniomaxillofac Surg: Official Publication of the European Association for Cranio-Maxillo-Facial Surgery 38: 589–594, 2010

Fletcher JW, Djulbegovic B, Soares HP, Siegel BA, Lowe VJ, Lyman GH, et al: Recommendations on the use of 18F-FDG PET in oncology. J Nucl Med: Official Publication, Society of Nuclear Medicine 49: 480–508, 2008

Guntinas-Lichius O, Wendt T, Buentzel J, Esser D, Lochner P, Mueller A, et al: Head and neck cancer in Germany: a site-specific analysis of survival of the Thuringian cancer registration database. J Cancer Res Clin Oncol 136: 55–63, 2010

Haerle SK, Strobel K, Ahmad N, Soltermann A, Schmid DT, Stoeckli SJ: Contrast-enhanced (1)(8)F-FDG-PET/CT for the assessment of necrotic lymph node metastases. Head Neck 33: 324–329, 2011

Herrmann K, Krause BJ, Bundschuh RA, Dechow T, Schwaiger M: Monitoring response to therapeutic interventions in patients with cancer. Semin Nucl Med 39: 210–232, 2009

Heusch P, Nensa F, Schaarschmidt B, Sivanesapillai R, Beiderwellen K, Gomez B, et al: Diagnostic accuracy of whole-body PET/MRI and whole-body PET/CT for TNM staging in oncology. Eur J Nucl Med Mol Imaging 42: 42–48, 2015

Higgins KA, Hoang JK, Roach MC, Chino J, Yoo DS, Turkington TG, et al: Analysis of pretreatment FDG-PET SUV parameters in head-and-neck cancer: tumor SUV-mean has superior prognostic value. Int J Radiat Oncol Biol Phys 82: 548–553, 2012

Hong HR, Jin S, Koo HJ, Roh JL, Kim JS, Cho KJ, et al: Clinical values of (18) F-FDG PET/CT in oral cavity cancer with dental artifacts on CT or MRI. J Surg Oncol 110: 696–701, 2014

Huang SH, Chien CY, Lin WC, Fang FM, Wang PW, Lui CC, et al: A comparative study of fused FDG PET/MRI, PET/CT, MRI, and CT imaging for assessing surrounding tissue invasion of advanced buccal squamous cell carcinoma. Clin Nucl Med 36: 518–525, 2011

Hustinx R, Lucignani G: PET/CT in head and neck cancer: an update. Eur J Nucl Med Mol Imaging 37: 645–651, 2010

Jemal A, Siegel R, Ward E, Murray T, Xu J, Thun MJ: Cancer statistics, 2007. CA Cancer J Clin 57: 43–66, 2007

Kim M, Achmad A, Higuchi T, Arisaka Y, Yokoo H, Yokoo S, et al: Effects of intratumoral inflammatory process on 18F-FDG uptake: pathologic and comparative study with 18F-fluoro-alpha-methyltyrosine PET/CT in oral squamous cell carcinoma. J Nucl Med: Official Publication, Society of Nuclear Medicine 56: 16–21, 2015

King AD: Multimodality imaging of head and neck cancer. Cancer Imaging: The Official Publication of the International Cancer Imaging Society 7(Spec No A): S37–S46, 2007

Kostakoglu L, Wong JC, Barrington SF, Cronin BF, Dynes AM, Maisey MN: Speech-related visualization of laryngeal muscles with fluorine-18-FDG. J Nucl Med: Official Publication, Society of Nuclear Medicine 37: 1771–1773, 1996

Kubiessa K, Purz S, Gawlitza M, Kuhn A, Fuchs J, Steinhoff KG, et al: Initial clinical results of simultaneous 18F-FDG PET/MRI in comparison to 18F-FDG PET/CT in patients with head and neck cancer. Eur J Nucl Med Mol Imaging 41: 639–648, 2014

Kurokawa T, Yoshida Y, Kawahara K, Tsuchida T, Okazawa H, Fujibayashi Y, et al: Expression of GLUT-1 glucose transfer, cellular proliferation activity and grade of tumor correlate with [F-18]-fluorodeoxyglucose uptake by positron emission tomography in epithelial tumors of the ovary. Int J Cancer Journal International du Cancer 109: 926–932, 2004

Levine ZH, Galloway BR, Peskin AP, Heussel CP, Chen JJ: Tumor volume measurement errors of RECIST studied with ellipsoids. Med Phys 38: 2552–2557, 2011

Nakamoto Y, Tamai K, Saga T, Higashi T, Hara T, Suga T, et al: Clinical value of image fusion from MR and PET in patients with head and neck cancer. Mol Imaging Biol: MIB: The Official Publication of the Academy of Molecular Imaging 11: 46–53, 2009

Nakamoto Y, Tatsumi M, Hammoud D, Cohade C, Osman MM, Wahl RL: Normal FDG distribution patterns in the head and neck: PET/CT evaluation. Radiology 234: 879–885, 2005

Platz H, Fries R, Hudec M, Min Tjoa A, Wagner RR: The prognostic relevance of various factors at the time of the first admission of the patient. Retrospective DOSAK study on carcinoma of the oral cavity. J Maxillofac Surg 11: 3–12, 1983

Quick HH, von Gall C, Zeilinger M, Wiesmuller M, Braun H, Ziegler S, et al: Integrated whole-body PET/MR hybrid imaging: clinical experience. Invest Radiol 48: 280–289, 2013

Reinbacher KE, Pau M, Wallner J, Zemann W, Klein A, Gstettner C, et al: Minimal invasive biopsy of intraconal expansion by PET/CT/MRI image-guided navigation: a new method. J Craniomaxillofac Surg: Official Publication of the European Association for Cranio-Maxillo-Facial Surgery 42: 1184–1189, 2014

Reske SN, Kotzerke J: FDG-PET for clinical use. Results of the 3rd German interdisciplinary consensus conference, "Onko-PET III", 21 July and 19 September 2000. Eur J Nucl Med 28: 1707–1723, 2001

Rodel R, Straehler-Pohl HJ, Palmedo H, Reichmann K, Jaeger U, Reinhardt MJ, et al: PET/CT imaging in head and neck tumors. Der Radiologe 44: 1055–1059, 2004

Rogers JW, Greven KM, McGuirt WF, Keyes Jr JW, Williams 3rd DW, Watson NE, et al: Can post-RT neck dissection be omitted for patients with head-and-neck cancer who have a negative PET scan after definitive radiation therapy? Int J Radiat Oncol Biol Phys 58: 694–697, 2004

Sadick M, Schoenberg SO, Hoermann K, Sadick H: Current oncologic concepts and emerging techniques for imaging of head and neck squamous cell cancer. GMS Curr Top Otorhinolaryngol Head Neck Surg 11(Doc08), 2012

Sham ME, Nishat S: Imaging modalities in head-and-neck cancer patients. Indian J Dent Res: Official Publication of Indian Society for Dental Research 23: 819–821, 2012

Stuck BA, Bachert C, Federspil P, Hosemann W, Klimek L, Mosges R, et al: Rhinosinusitis guidelines–unabridged version: S2 guidelines from the German Society of Otorhinolaryngology, Head and Neck Surgery. HNO 60: 141–162, 2012

Subramaniam RM, Truong M, Peller P, Sakai O, Mercier G: Fluorodeoxyglucose-positron-emission tomography imaging of head and neck squamous cell cancer. AJNR Am J Neuroradiol 31: 598–604, 2010

Wolff KD, Follmann M, Nast A: The diagnosis and treatment of oral cavity cancer. Dtsch Arzteblatt Int 109: 829–835, 2012

Xiao Y, Chen Y, Shi Y, Wu Z: The value of fluorine-18 fluorodeoxyglucose PET/MRI in the diagnosis of head and neck carcinoma: a meta-analysis. Nucl Med Commun 36: 312–318, 2015

Yaghmai V, Miller FH, Rezai P, Benson 3rd AB, Salem R: Response to treatment series: part 2, tumor response assessment–using new and conventional criteria. AJR Am J Roentgenol 197: 18–27, 2011

Yamashina A, Tanimoto K, Sutthiprapaporn P, Hayakawa Y: The reliability of computed tomography (CT) values and dimensional measurements of the oropharyngeal region using cone beam CT: comparison with multidetector CT. Dentomaxillofac Radiol 37: 245–251, 2008

Zienolddiny S, Aguelon AM, Mironov N, Mathew B, Thomas G, Sankaranarayanan R, et al: Genomic instability in oral squamous cell carcinoma: relationship to betel-quid chewing. Oral Oncol 40: 298–303, 2004

Zinreich SJ, Kennedy DW, Rosenbaum AE, Gayler BW, Kumar AJ, Stammberger H: Paranasal sinuses: CT imaging requirements for endoscopic surgery. Radiology 163: 769–775, 1987